The solid-solid-liquid triple line and its effect on the grain structure of multi-crystalline photovoltaic silicon

Thierry Duffar, Amal Nadri

The grain–grain–liquid triple phase line during solidification of multi-crystalline silicon

La ligne triple grain–grain–liquide lors de la solidification du silicium multi-cristallin

Thierry Duffar *, Amal Nadri

SIMaP–EPM, Grenoble-INP–CNRS–UJF, BP 75, 38402 Saint Martin d'Héres cedex, France

The rough or faceted morphology of the solid–liquid interface during solidification of multi-crystalline silicon is discussed in terms of classical crystallographic, energetic and kinetic considerations. This allows establishing diagrams of the interface structure as a function of process parameters. It is shown that the grain–grain–liquid triple phase line structures determine quantitatively the direction of growth of the grain boundaries, then opening the door to the numerical modeling of the grain structure of photovoltaic silicon ingots as a function of growth conditions.

La morphologie, facettée ou rugueuse, de l'interface solide–liquide lors de la solidification du silicium multi-cristallin est discutée sur la base de considérations cristallographiques, énergétiques et cinétiques classiques. Ceci permet d'établir des diagrammes donnant la structure de l'interface de solidification en fonction des paramètres du procédé. On montre que la structure des lignes triples grain–grain–liquide détermine la direction des joints de grains de façon quantitative, ce qui permet d'envisager la modélisation numérique de la structure de grains de lingots de silicium photovoltaïque en fonction des conditions de croissance.

1. Introduction

The grain structure of multi-crystalline Si ingots impacts the conversion efficiency of photovoltaic cells, because grain boundaries are location of lattice defects that interact with minority carriers [1,2]. Furthermore, grain boundaries act as getters that attract impurities, which has the drawback of increasing the grain boundary electrical effect but the advantage of cleaning the surrounding grains. These effects have gained importance as industry uses less pure silicon raw material [3].

It is therefore important to know how the grain structure develops in Si multi-crystalline ingots. This topic has been studied for a long time (see a review in [4]) and the multi-silicon structure is typically composed of three types of grains:

* Corresponding author.
E-mail address: thierry.duffar@grenoble-inp.fr (T. Duffar).

Table 1
Selection of surface energy values for Si interfaces.

Tableau 1
Une sélection de valeurs des énergies de surface dans le cas du silicium.

Interface type	Surface energy	References
Solid–liquid[a]	0.4 to 0.68 $\mathrm{J\,m^{-2}}$	[16,17]
Solid–liquid step energy	0.087 $\mathrm{J\,m^{-1}}$	[18]
Solid–solid $\Sigma 3$ twin	Theory: 0.026 to 0.077 $\mathrm{J\,m^{-2}}$ Experiments: 0.060 $\mathrm{J\,m^{-2}}$	[19]
Solid–solid $\Sigma 9$ twin	0.64 $\mathrm{J\,m^{-2}}$	[20]
Random grain boundary	1.3 $\mathrm{J\,m^{-2}}$	[19]
Grain boundary twisted around ⟨110⟩ or ⟨100⟩ axis	From 0.6 to 1.3 $\mathrm{J\,m^{-2}}$ (except for $\Sigma 3$ twin)	See plots in [21,22]

[a] Ref. [23] reports that anisotropy is less than 15% in the order {111} < {110} < {100}. This is confirmed by numerical simulation [24].

- Long columnar grains with a diameter of the centimeter order, which develop along the growth direction. This is the preferred structure because grains are large and do not impact very much on the properties.
- Small equiaxed grains of millimeter size. They should be avoided as they decrease the photovoltaic efficiency and are associated with SiC precipitates that induce severe problems during subsequent wafering. They have been shown to be related to the nucleation of Si on SiC precipitates [5], when C pollution occurs, but this needs a significant undercooling of the solid–liquid interface during growth, at least 0.1 K [6].
- $\Sigma 3$ twins that are not electrically active by themselves but, when crossing or multiplying, produce $\Sigma 9$, $\Sigma 27$, etc. boundaries. It has been shown that four levels of successive twinning result in a random structure of incoherent grains [7]. The same authors have measured that two cell wafers cut from a directionally solidified ingot are composed of only 50 to 60% of random grains, the remaining grain boundaries being of the type $\Sigma 3^n$. This result has been confirmed in the case of a Si ingot grown by cold crucible continuous casting, under much higher growth rate and thermal gradient [8], demonstrating the importance of twinning in photovoltaic Si solidification. A mechanism of twinning in multi-crystalline Si has been proposed recently [9], based on the existence of undercooled facets at the interface.

It follows that the grain structure in multi-crystalline silicon largely depends on a series of phenomena related to faceting/undercooling of the solid–liquid interface during growth. This paper discusses the solid–liquid interface structure based on the morphology of the grain–grain–liquid triple lines. Very classical kinetic and energetic considerations are used. The most important is that, according to the Jackson criterion [10] and as demonstrated in many occasions, facets in Si are only of the {111} family. Ref. [11] reports possible {110} facets, but this is still to be confirmed.

Growth kinetics in Si are well known:

- In the case of a rough interface, the relationship between the interface growth velocity, V_I, and the undercooling, ΔT, is linear; for the ⟨100⟩ direction, [12,13] give:

$$V_{I\{100\}} \approx 0.12\Delta T \quad \left(\text{in m s}^{-1} \text{ and K}\right) \tag{1}$$

  which gives an undercooling of 10^{-4} K for a typical solidification rate of 10 $\mu\mathrm{m\,s^{-1}}$.
- In the case of a faceted {111} interface where two-dimensional nucleation occurs, [14] has reviewed the existing literature and proposes the relation:

$$V_F = 0.04956 e^{-\frac{46.67}{\Delta T}} (0.3\Delta T)^{2/3} \quad \left(\text{in m s}^{-1} \text{ and K}\right) \tag{2}$$

  which gives an undercooling of 5 K for a typical solidification rate of 10 $\mu\mathrm{m\,s^{-1}}$.
- In the case of a faceted {111} interface with unsaturable steps (for example due to dislocations), [15] proposed the relation:

$$V_F \approx 0.3 \times 10^{-3} \Delta T^2 \quad \left(\text{in m s}^{-1} \text{ and K}\right) \tag{3}$$

  which gives an undercooling of 0.2 K for a typical solidification rate of 10 $\mu\mathrm{m\,s^{-1}}$.

From the energetic point of view, Table 1 gives a selection of interfacial energies in Si, relevant to our considerations. It can be seen that, except for the $\Sigma 3$ twin, the grain boundaries have similar energies, whatever their relative mis-orientation. Bristowe [19], in a review of molecular dynamics and quantum mechanics simulations, shows that an amorphous layer, 0.25 nm thick, exists between twist grains. The energy of tilt grains is lower and it is not clear whether pre-melting exists at grain boundaries close to the melting point in this case. Following [25], it is likely that only the $\Sigma 3$ boundary remains crystalline close to the melting point. In the following, it will be considered that, for all other boundaries, the phenomena occurring on one side of the groove are not influenced by what happens on the other side.

In the second part, the morphology of the boundary surrounding a single grain will be discussed. This will allow, in the third part, a simple computation of the faceted or rough structure of the solid–liquid interface as a function of the growth

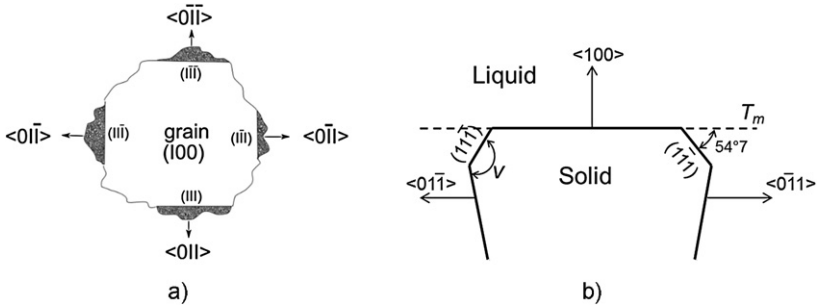

Fig. 1. A ⟨100⟩-orientated grain has four facets all around its grain boundary, each of them corresponding to a [011] direction. (a) Seen from the melt; (b) cut along the ⟨0$\bar{1}$1⟩ direction.

Fig. 1. Un grain orienté ⟨100⟩ présente 4 facettes sur sa frontière, chacune dans une des directions ⟨011⟩. (a) Vu depuis le liquide ; (b) vu en coupe suivant la direction ⟨0$\bar{1}$1⟩.

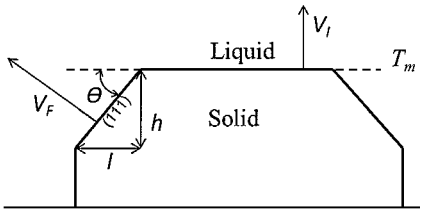

Fig. 2. Calculation of the facet size.

Fig. 2. Calcul de la taille d'une facette.

parameters. Several types of Grain–Grain–Liquid Triple Phase Lines (GGL-TPL) will be presented in the fourth part and it will be shown that each of them induces a particular orientation of the grain boundary toward the solid–liquid interface.

2. Conditions for grain boundary faceting

The morphology of the GGL-TPL will depend on whether the interface is rough or faceted at the TPL.

In order for the boundary of one grain to be faceted, there is first a crystallographic criterion: as facets are necessarily {111} planes, they can only exist on some parts of the grain boundary around one grain. Fig. 1 shows the case of a grain which is growing in the ⟨100⟩ direction, for the sake of simplicity. It can be seen that the four possible {111} facets can be found in the [011] directions only. In this case the facets make an angle of 54.7° with the (100) plane, i.e. with the solid–liquid isotherm, T_{fus}. More generally, the locations of facets around a grain depend on the orientation of the grain relatively to the normal to the solid–liquid isotherm: a ⟨100⟩-orientated grain will show 4 facets, a ⟨110⟩-orientated grain will show two facets (at 35.3° from the solidification isotherm), a ⟨111⟩-orientated grain will show one facet parallel to the solidification isotherm and three facets at the grain boundary (at 70.5° from the solidification isotherm), and so on.

There is also an energetic criterion: following [26] a facet is possible only if the energy of the system decreases when a growing step reaches the facet boundary. This gives a condition on the angle, ν, between the facet and the grain boundary (see Fig. 1-b). As shown in [9], this angle should be in the range [93°–176°], which range depends on the values chosen for the step, facet–liquid and solid–liquid surface energies (see Table 1).

3. Proportion of facets as a function of growth conditions

In order to grow upwards with the same velocity, V_I, as the displacement rate of the melting isotherm, T_m, the facet velocity, V_F, should be (see Fig. 2):

$$V_F = \frac{V_I}{\cos\theta} \tag{4}$$

For a non-dislocated grain, the facet undercooling, ΔT, depends on the facet velocity, V_F, through Eq. (2) (for a dislocated grain, Eq. (3) should be used). This undercooling gives the temperature of the coldest part of the facet, which means that the facet size, l, can be calculated as a function of the temperature gradient at the solid–liquid interface, G_{th}:

$$l = \frac{h}{\tan\theta} = \frac{\Delta T(V_F)}{G_{th}\tan\theta} \tag{5}$$

If the facet size is larger than the half width of the grain, the grain will be totally faceted. Consequently, for a given grain size, there are growth conditions, V_I and G_{th}, under which the solid–liquid interface is totally faceted. Fig. 3 is a velocity-

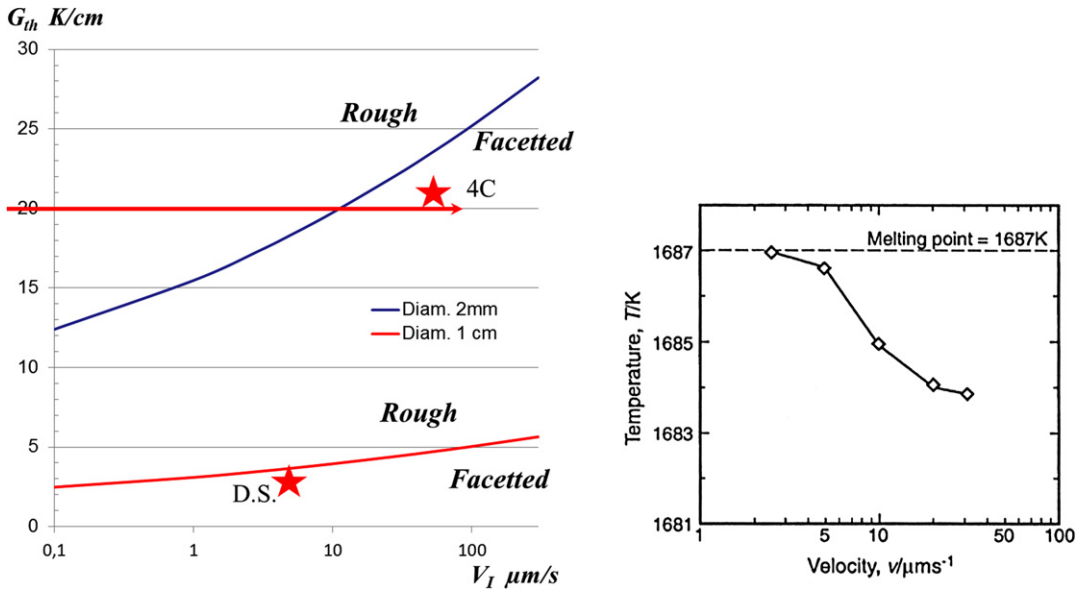

Fig. 3. Diagram showing the growth conditions under which the solid–liquid interface is fully faceted. Temperature measurements by [27] are shown on the right and have been performed along the horizontal arrow for 2 mm grains. Stars show the operating conditions of the DS and 4C processes.

Fig. 3. Carte montrant les conditions de croissance sous lesquelles l'interface est facettée. Les mesures de températures de [27] sont montrées à droite et ont été réalisées suivant la flèche horizontale. Les étoiles montrent les conditions opératoires des procédés DS et 4C.

gradient diagram, plotted from Eqs. (2), (4) and (5) with a mean angle $\theta = 54.7°$, which gives the transition between a fully faceted and a partially faceted interface, for two grain sizes: 2 mm, typical of the structure obtained by Cold Crucible Continuous Casting (4C), and 1 cm, as obtained by Directional Solidification (DS).

The horizontal arrow, for a gradient of 20 $\mathrm{K\,m^{-1}}$, represents Miyahara's experiments [27], in which the temperature of the solid–liquid interface has been measured with a thermocouple, as a function of the growth rate. For a low growth rate the interface undercooling was negligible, showing a mainly rough interface, and it increased up to 3 K for large velocities, showing a mainly faceted interface. Their grain size was about 2 mm and the agreement with Fig. 3 is surprisingly good. This supposes that their sample did not show dislocation, which is supported by the large measured undercooling.

It can be seen that the two growth techniques, DS and 4C, whose typical growth conditions are represented by stars in the figure, fall into the faceted region: this explains why so much twins can be seen and measured in these wafers [7,8], as twinning can only occur in the presence of facets. This also explains why equiaxed grains occur in these processes as soon as significant carbon allows SiC precipitation, because nucleation of Si on the SiC necessitates undercooling which is provided by the facets. The diagram presented in Fig. 3 is quite rough because it does not take into account crystallographic details or the real kinetic of a faceted GGL-TPL. In case of a preferred orientation of the grains, the angle θ should be adjusted accordingly and, for a given process, it will be possible to include more detailed kinetic considerations (see Section 4).

4. The four possible configurations of the GGL-TPL

As seen in Section 2, the boundary around one grain can be faceted or rough, depending on the crystallographic orientation and conditions. Consequently, when two grains are facing in order to build a grain boundary, three configurations are possible.

(1) When two rough boundaries are facing, it gives a Rough-TPL, see Fig. 4, bottom, and Fig. 5. This situation is very well known in the solidification of metallic alloys. The model developed by Bolling [28] has been applied to the case of Si [9], and has given a groove height of 17 micrometers which gives an undercooling $\Delta T = 0.017$ K (for $G_{th} = 1000$ $\mathrm{K\,m^{-1}}$) at the groove bottom: clearly these values are negligible. As in the case of metals, the grain boundary angle to the growth direction, ϕ, is dictated by the kinetic coefficients k_1 and k_2 of the two grains, which depend on their orientations θ_1 and θ_2 toward the growth direction (Fig. 5):

$$\varphi = \frac{\pi}{2} - \arcsin\left(\frac{k_1(\theta_1)}{k_2(\theta_2)}\right) \tag{6}$$

Some data are available in the case of Si, Atwater [29] gives $\frac{k_{\langle 100\rangle}}{k_{\langle 110\rangle}} = 1.2$, and Steinbach [30] uses $\frac{k_{\langle 100\rangle}}{k_{\langle 111\rangle}} = 1.5$, with $k_{\langle 111\rangle}$ the kinetic coefficient of surfaces close to {111}.

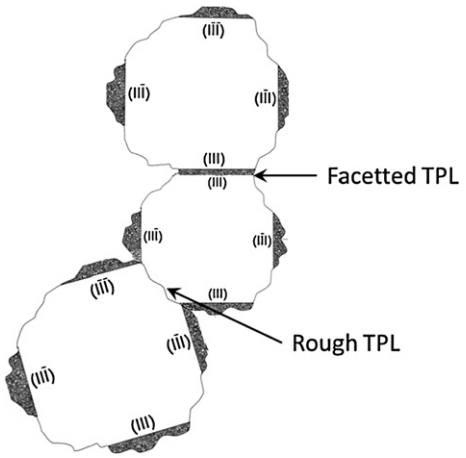

Fig. 4. Three grains (all ⟨100⟩-orientated) seen from the liquid, giving a Rough-TPL and a Faceted-TPL.
Fig. 4. Trois grains (tous supposés d'orientation ⟨100⟩) vus depuis le liquide, montrant des lignes triples rugueuse et facettée.

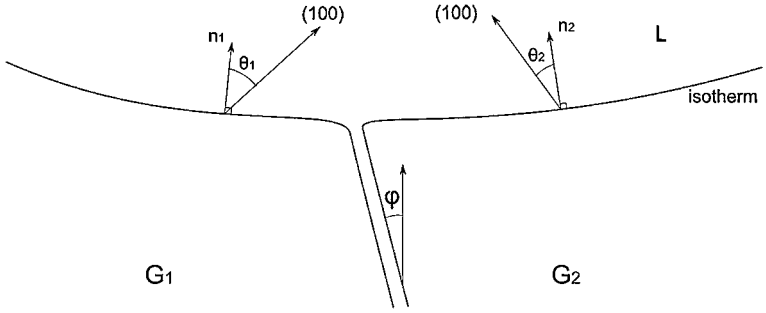

Fig. 5. The growth configuration of the Rough-TPL.
Fig. 5. Configuration de croissance d'une ligne triple rugueuse.

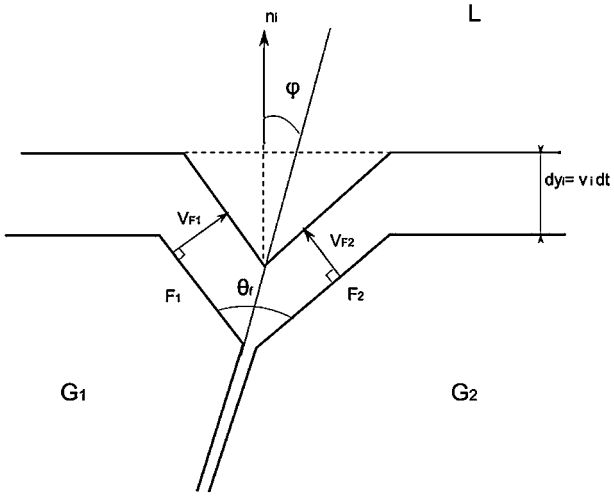

Fig. 6. The growth configuration of the Faceted-TPL.
Fig. 6. Configuration de croissance d'une ligne triple facettée.

(2) When two facets are facing, this gives a Faceted-TPL, see Fig. 4, top, and Fig. 6. This configuration has been observed at the surface of EFG ribbons, where marking of the solid–liquid interface occurs because of pulling shaft vibrations [31,32]. Interface marking during Bridgman growth of multi-crystalline GaSb has also shown Faceted-TPL [33].

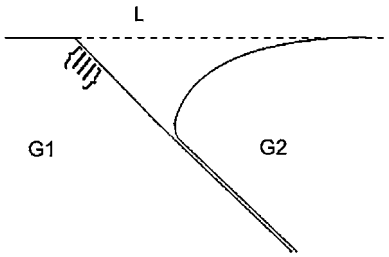

Fig. 7. The growth configuration of the Rough-Faceted-TPL.

Fig. 7. Configuration de croissance d'une ligne triple rugueuse-facettée.

It is clear that the undercooling at the bottom of the groove is maximum and the same for both facets. Therefore they should have the same facet velocity, V_F, and the grain boundary angle φ toward the growth direction n_I should follow the bisector of the angle between the two facets, θ_f: It depends only on the crystallographic orientation of the two grains. From Fig. 6, considering that the groove bottom moves up at the velocity V_I, it comes:

$$V_F = \frac{V_I \sin(\theta/2)}{\cos(\varphi)} \tag{7}$$

This allows, through Eq. (2) or Eq. (3), computing the undercooling and then the groove height. In the case where there is no step source on the facet, the undercooling is of the order of 4 K under typical growth conditions, and the groove can be one centimeter deep or even more. When Eq. (3) is used, the groove depth is of the millimeter order, which is in agreement with experimental results [34].

(3) When a facet is facing a rough boundary, it gives a Rough-Faceted-TPL, Fig. 7. The rough side fixes a low undercooling at the groove bottom, always smaller than 0.1 K, as computed from [28], which makes nucleation of 2D seeds on the faceted side very rare. Therefore the facet cannot move significantly and the grain boundary simply follows the {111} facet. This configuration has been observed experimentally by Börzönyi [35] in the case of the nematic–smectic faceted interface in C_4H_9–$(C_6H_{10})_2CN$: the facet moved very slowly compared to the growth rate.

(4) A fourth configuration of TPL concerns the intersection of a $\Sigma 3$ twin boundary with the solid–liquid interface. Crystallographic relationships show that it belongs to the Faceted-TPL but with the particularity that this twin boundary is the only one that does not present an amorphous layer between the solid grains. Its surface energy is much lower than any other solid–solid boundary, so that it necessarily grows always in the same direction, giving the well-known straight boundaries that can be observed on any multi-crystalline Si solar cell. In spite of the fact that it shows a Faceted-TPL, there is no chance that twinning occurs on these facets, because this would create another $\Sigma 3$ twin boundary plus a $\Sigma 9$ boundary, which is totally unlikely from the energetic point of view.

5. Conclusion

The morphology of the grain–grain–liquid triple phase line in multi-crystalline Si has been discussed on the basis of classical kinetic, energetic and crystallographic considerations.

It has been shown that the TPL can be faceted under given conditions and that the facets are likely to overrun the whole solid–liquid interface, especially under relatively high growth rates and low temperature gradients. This enhances the occurrence of twinning and equiaxed growth and therefore importantly controls the grain structure of the ingot.

When two grains are facing, the TPL can show faceted or rough sides, which gives three different configurations, each of them with its particular grain boundary orientation law. The $\Sigma 3$ twin boundary is a particular case also taken into account. In summary:

- When the TPL is rough on both sides, the grain boundary orientation results from the kinetics of the two grains (as in classical metallurgy);
- When the TPL is faceted on both sides, the grain boundary orientation is the bisector of the two facets;
- When the TPL is rough on one side and faceted on the other, the grain boundary follows the facet direction;
- When the TPL results from a $\Sigma 3$ twin boundary, the grain boundary follows the twin plane.

This opens the possibility to predict the grain structure in the Si ingot, in the case of pure material. The next step of this research will be the development of a two-dimensional simulation software in order to model the structure of a Si ingot as a function of the growth conditions. Further development could include 3D simulation but a severe limitation is that it should take into account not only the direction of the grain boundaries, but also the behavior of the grain–grain–grain triple lines during growth, which is totally unknown at the moment and should deserve further research.

On the experimental point of view, there is a need to check the validity of the proposed model and to feed it with appropriate physical properties, especially kinetic coefficients as a function of orientation. In situ observation of the solid–

liquid interface morphology by synchrotron X-ray densitometry is aiming to check the model and has already confirmed the existence of the Faceted-TPL during Si growth, see the paper published in the same issue of this journal [34].

It is worth to notice that the structure of a given TPL is likely to evolve during the growth process, because the growth conditions, or the orientation of the solid–liquid interface, are changing. Also, multiplication of dislocations with time can have a very strong effect on the facet sizes and then on the evolution of TPL structures. Therefore a Faceted-TPL may become a Rough-TPL and vice versa.

Considering further improvements of the model, impurity effect should be added. This could be through modifications of surface energies, but also by taking into account interface destabilization. Finally the reader should keep in mind that grain boundaries can also be generated in the solid state, through dislocation aggregation or mechanical twinning, phenomena which have not been taken into account here.

Acknowledgements

This research has been supported by the ANR-HABISOL-SiX and the OSEO-SNC research projects and through a PhD grant of the MESR attributed in the frame of Grenoble-INP BQR. Authors acknowledge the constructive help and discussions of Prof. D. Bellet, their colleagues of IM2NP-Marseille and the whole Si-X team.

References

[1] T.F. Ciszek, T.H. Wang, R.W. Burrows, X. Wu, J. Alleman, T. Bekkedahl, Y.S. Tsuo, in: Proc. 23rd PV Specialist Conf., Louisville, KY, IEEE 0-7803-1220-1, 1993, pp. 101–105.
[2] J. Nelson, The Physics of Solar Cells, Imperial College Press, London, ISBN 1-86094-340-3, 2003.
[3] S. Dubois, PhD thesis, Univ. Paul Cézanne-Marseille III, 2007 (in French).
[4] T. Duffar, Recent Res. Devel. Cryst. Growth 5 (2010) 61–111.
[5] N. Mangelinck-Noel, T. Duffar, J. Cryst. Growth 311 (2008) 20–25.
[6] M. Beaudhuin, T. Duffar, M. Lemiti, K. Zaidat, J. Cryst. Growth 319 (2011) 106–113.
[7] A. Voigt, E. Wolf, H.P. Strunk, Mater. Sci. Eng. B 54 (1998) 202–206.
[8] B. Gallien, Th. Duffar, S. Lay, F. Robaut, J. Cryst. Growth 318 (2011) 208–211.
[9] T. Duffar, A. Nadri, Scr. Mater. 62 (2010) 955–960.
[10] K.A. Jackson, in: Liquid Metals and Solidification, ASM, Cleveland, 1958, pp. 174–186.
[11] P. Rudolph, M. Czupalla, B. Lux, F. Kirscht, Ch. Frank-Rotsch, W. Miller, M. Albrecht, J. Cryst. Growth 318 (2011) 249–254.
[12] K.M. Beatty, K.A. Jackson, J. Cryst. Growth 211 (2000) 13–17.
[13] D. Buta, M. Asta, J.J. Hoyt, J. Chem. Phys. 127 (2007) 074703.
[14] W. Miller, J. Cryst. Growth 325 (2011) 101–103.
[15] V.V. Voronkov, Sov. Phys. Crystallogr. 17 (1973) 807–813 (trans. from Kristallografiya 17 (1972) 909–917).
[16] R.P. Liu, T. Volkmann, D.M. Herlach, Acta Mater. 49 (2001) 439–444.
[17] Z. Jian, K. Kuribayashi, W. Jie, F. Chang, Acta Mater. 54 (2006) 3227–3232.
[18] D.T.J. Hurle, J. Cryst. Growth 147 (1995) 239–250.
[19] P.D. Bristowe, in: R. Hull (Ed.), Properties of Crystalline Si, EMIS, 1999, pp. 299–308.
[20] A.V. Artemyev, L.E. Polyak, L.K. Fionova, J. Phys., Colloq. 51 (1990) C1/71–C1/76.
[21] M. Kohyama, R. Yamamoto, M. Doyama, Phys. Status Solidi (b) 138 (1986) 387–397.
[22] A. Otsuki, Acta Mater. 49 (2001) 1737–1745.
[23] H. Sens, PhD thesis, Institut National Polytechnique de Grenoble, 1988 (in French).
[24] P. Apte, X.C. Zeng, Appl. Phys. Lett. 92 (2008) 221903.
[25] L. Priester, Les joints de grains, de la théorie à l'ingénierie, EDP Sciences, Paris, 2006 (in French).
[26] V.V. Voronkov, Sov. Phys. Crystallogr. 19 (1975) 573–577 (trans. from Kristallografiya 19 (1974) 922–929).
[27] H. Miyahara, S. Nara, M. Okugawa, K. Ogi, Mater. Trans. 5 (2005) 935–943.
[28] G.F. Bolling, W.A. Tiller, J. Appl. Phys. 31 (1960) 1345–1350.
[29] H.A. Atwater, C.V. Thompson, H.I. Smith, J. Mater. Res. 3 (1988) 1232–1237.
[30] I. Steinbach, F. Pezzolla, R. Prieler, in: M. Cross, J. Campbell (Eds.), 7th MCWASP Proc., The 3M Soc., 1995, pp. 695–703.
[31] T. Surek, C.B. Hari Rao, J.C. Swartz, L.C. Garone, J. Electrochem. Soc. 124 (1977) 112–123.
[32] E.A. Katz, L.E. Polyak, J. Cryst. Growth 172 (1997) 115–119.
[33] A. Mitric, PhD thesis, Grenoble Institute of Technology, 29 May 2006 (in French).
[34] A. Tandjaoui, N. Mangelinck-Noel, G. Reinhart, B. Billia, X. Guichard, C. R. Physique 14 (2013), in this issue, http://dx.doi.org/10.1016/j.crhy.2012.12.001.
[35] T. Börzönyi, S. Akamatsu, Phys. Rev. E 66 (2002) 051709.